ACS OMEGA

http://pubs.acs.org/journal/acsodf

Article

Preparation and Properties of Epoxy/Multiwalled Carbon Nanotube Nanocomposite Foams with an Alternating Layer Structure

Shaohua Sun,* Lijun Wang, and Bin Xue

Cite This: *ACS Omega* 2022, 7, 33010−33018

Read Online

ACCESS | Metrics & More | Article Recommendations

ABSTRACT: Multilayered epoxy/multiwalled carbon nanotube (EP/MWCNT) composite foams with a density of 0.713 g/cm^3 were prepared through the chemical foaming of laminated epoxy sheets in a mold with a fixed cavity. The difference in cell morphology and properties between adjacent layers in the multilayer foams (two- and four-layer) was tuned by MWCNT or chemical foaming agent (CFA) concentration. It was found that the storage modulus and microwave-absorbing ability of the multilayered EP/MWCNT foams were strongly associated with the loading direction, the thermal diffusivity was slightly direction-dependent, and the electromagnetic interference (EMI) shielding effectiveness (SE) was direction-independent. In addition, as the layer number increased, the mechanical, thermal, and electrical conductivity properties and EMI shielding performances of the multilayered composite foams showed different change tendencies. These results indicated that the effect of the multilayer structure on the properties of composite foams was different when they underwent force, heat, or electromagnetic microwave, and the underlying reasons were investigated in detail.

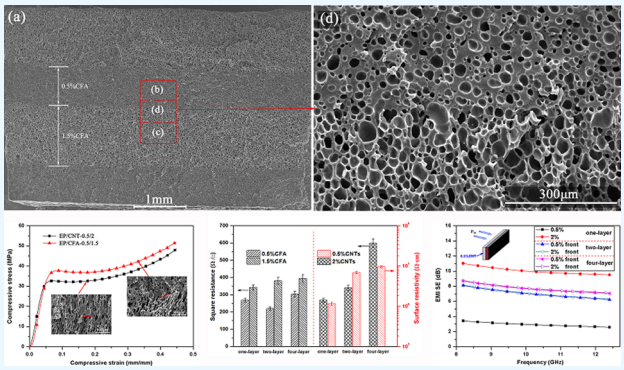

1. INTRODUCTION

Conductive polymer composites (CPCs), which are prepared by incorporating conductive fillers into a polymer matrix, have attracted great interest as a potential substitute for metals applied in the electronics industry due to their lightweight, flexible, easy processing, and resistance to corrosion.[1−3] As compared with metal powders, carbon nanomaterials like carbon nanotubes (CNTs) and graphene have outstanding structural and electrical properties, and thereby have emerged as an attractive option for conductive composite materials.[2,4−9] Further, making these CPCs into a porous structure will bring added advantages, including savings in materials and energy, easier manipulation, and lower electrical percolation threshold,[6,10] which is of great significance for electronic devices, especially those used in aircraft, watercraft, and automobiles.

In contrast to the monolayer foams with a homogeneous cellular structure, multilayered composite foams can be designed to further improve the properties of the electromagnetic wave-absorbing and -soundproofing materials.[11−15] Conventionally, the preparation of multilayered composite foams involves the processes of stacking and foaming. Li et al.[12] fabricated multilayered thermoplastic polyurethane/graphene (PUG) composites by stacking single-layered PUG foams together, which was proved to be a facile approach to enhance the microwave-absorbing property of PUG composites. The graphene concentration, cell morphology, and thickness of each layer can be freely tailored in this method, but the discontinuous interface between adjacent layers brings drawbacks to the application. On the contrary, first stacking different sample sheets together by hot melt pressing or multilayer coextrusion and then foaming these laminated sheets is a feasible and convenient technology to obtain multilayered foams with a continuous interface.[11,13−17] For example, Zhao et al.[14] prepared a poly(ethylene-*co*-octene) composite with a foam/film alternating multilayered structure through a multilayered coextrusion system. They found that the average cell size decreased and the sound absorption efficiency of the multilayered foams increased with increasing the layer number. Zhou et al.[16] prepared poly(methylmethacrylate) (PMMA) foams with a multilayer cell structure via the combination of melt hot pressing and physical supercritical CO_2 foaming method. When the distance of the multilayer interface was smaller than the critical nucleation size of the cell, the PMMA foams with uniform, continuous, and

Received: May 2, 2022
Accepted: September 2, 2022
Published: September 12, 2022

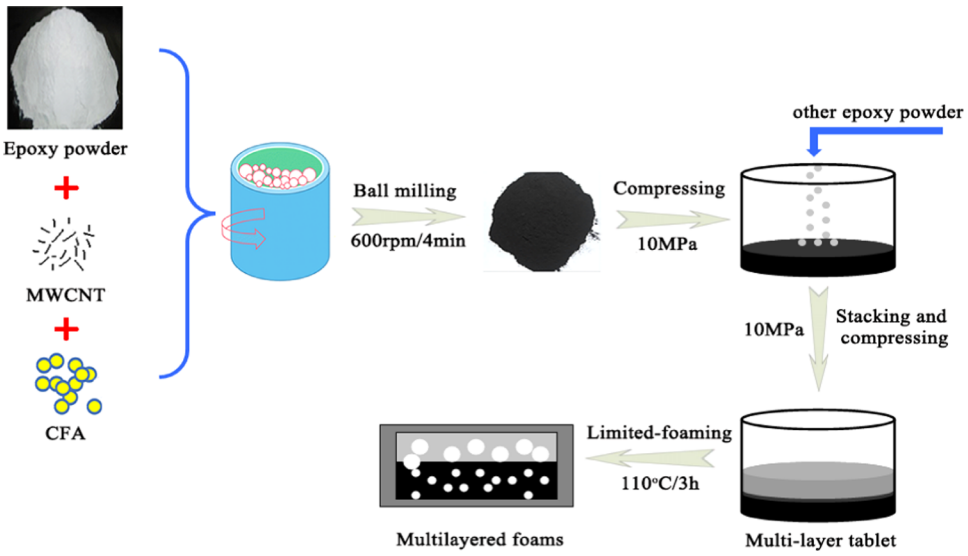

Figure 1. Schematic of the fabrication of multilayered epoxy composite foams.

directional multilayer cell structure were obtained. However, tuning the cell structure in each layer still remains challenging in this literature, and thereby the effect of different cell morphologies between adjacent layers on the properties of the multilayered composite foams is scarcely reported.[11]

Considering that epoxy resin exhibits excellent properties, including strong adhesion, good thermal and chemical stability, and low toxicity, the application of epoxy resin for preparing conductive composite foams has been extensively reported.[18−24] For example, Fan et al.[18] prepared highly expansive epoxy/silver nanosheet (EP/AgNS) composite foams through a batch foaming process with supercritical CO_2. Multiproperties including an electrical conductivity of 89.12 S/m, a specific electromagnetic interference (EMI) shielding effectiveness (SE) of 334.59 dB·cm^3/g, and a thermal conductivity of 58.71 mW/m·K were achieved in the epoxy composite foam with 20 wt % AgNS. Yang et al.[21] prepared epoxy/nickel-coated carbon fiber (EP/NCCF) conductive foams via chemical foaming. The composite foams exhibited a specific EMI SE of as high as 77.4 dB·cm^3/g in the X-band at a density of 0.45 g/cm^3 by adding 5.03 vol % of NCCFs. However, epoxy-based conductive foams with alternating multilayer cell structures have not been reported yet.

In this study, microcellular epoxy/multiwalled carbon nanotube (EP/MWCNT) composite foams with alternating layer structures were prepared through the combination of multilayer powder pressing and chemical foaming technology. We investigated the foaming behavior of the two- and four-layer composite foams with different contents of MWCNT or the chemical foaming agent (CFA) in the adjacent layers and attempted to correlate the multilayer structure with the mechanical, electromagnetic interference shielding, and electrically and thermally conductive properties.

2. EXPERIMENTAL SECTION

2.1. Materials. Diglycidyl ether of bisphenol-A epoxy resin (DGEBA, epoxy value = 0.51 mol/100 g), hardener methyl-5,6-dihydro-4*H*-isobenzofuran-1,3-dione (MeTHPA), and 2,4,6-tris(dimethylaminomethyl)phenol (DMP-30) used as curing aids were supplied by Shanghai Resin Company, China. Multiwalled carbon nanotubes (MWCNTs, carbon purity >99%) with a diameter of 10−30 nm and an average length of 10−30 μm were supplied by Chengdu Organic Chemicals Institute, Chinese Academy of Sciences. The chemical foaming agent (CFA) was 3,7-dinitroso-1,3,5,7-tetraazobicyclo-nonane, which was purchased from Guangzhou Longsun Technology Company, China.

2.2. Sample Preparation. Epoxy powder was prepared according to the literature.[24] Briefly, epoxy resin and a stoichiometric amount of MeTHPA were mixed well, and thereafter the mixture was thoroughly stirred at 85 °C for precuring. When the torque of the mixture reached 0.04 dN·m, it was quickly cooled to room temperature, and then the brittle monolith was crushed into powder.

The fabrication of multilayered epoxy nanocomposite foams is illustrated in Figure 1. First, the MWCNTs (0.5 or 2 wt % epoxy powder) and CFA (0.5 or 1.5 wt % epoxy powder) were mixed with the epoxy powder in a ball-milling apparatus at a speed of 600 rpm for 4 min to obtain different hybrid powders. Second, two different hybrid powders were compressed layer by layer through a tablet machine under 10 MPa at room temperature, and thereafter the tablets (diameter = 35 mm) with alternating layer structures were obtained. The weight of each layer in a laminated sheet was the same, and the total weight of the tablets was fixed at 2.8 g, irrespective of the layer number. Third, these tablets were loaded in a preheated mold with a fixed cavity of 35.5 mm × 4 mm (diameter and height, respectively), foamed at 110 °C for 3 h, and postcured at 150 °C for 2 h and 220 °C for 2 h, respectively. Since the cavity of the mold was smaller than the volume of the tablet foamed in free space, the growth of bubbles was restricted before the growth ended. Therefore, the density of all of the composite foams in this study was about 0.713 g/cm^3 due to the fixed weight of tablets and foaming space. Two kinds of multilayered composite foams were prepared and named EP/CNT-0.5/2 and EP/CFA-0.5/1.5, respectively. The adjacent layer in the EP/CNT-0.5/2 foam contained 0.5 and 2 wt % MWCNT, respectively, while that in the EP/CFA-0.5/1.5 foam contained 0.5 and 1.5 wt % CFA. The CFA content in the EP/CNT-0.5/2 foam was fixed at 0.5 wt %, while the MWCNT content in the EP/CFA-0.5/1.5 foam was fixed at 2 wt %.

https://doi.org/10.1021/acsomega.2c02710
ACS Omega 2022, 7, 33010−33018

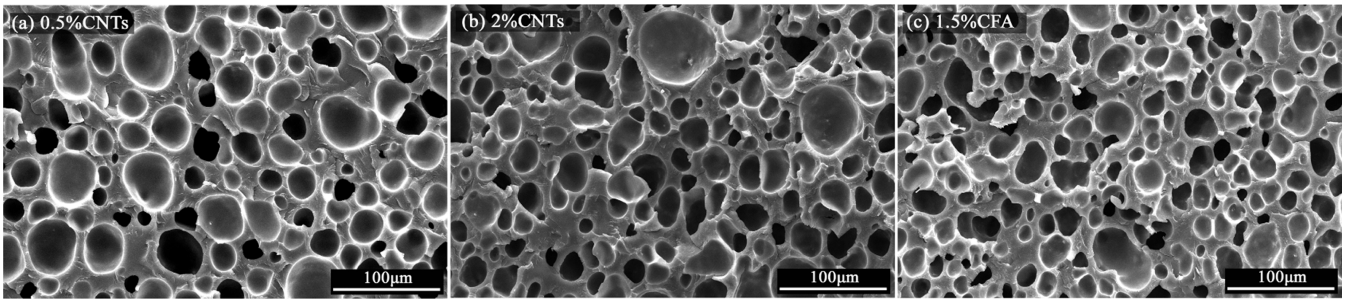

Figure 2. SEM micrographs of monolayer epoxy foams. The CFA content of samples (a, b) was 0.5 wt % and the MWCNT content of sample (c) was 2 wt %.

2.3. Characterization. *2.3.1. Morphological Analysis.* A field emission scanning electron microscope (SEM, FEI), QUANTA FEG 250, was used to observe the microstructures of the epoxy composite foams. Fractured surfaces were sputter-coated with gold for SEM observation. The cell size and cell density were obtained by image analysis using software Image-Pro. The cell density (N_f) was determined by the number of cells per unit volume of foam, which was calculated using eq 1

$$N_f = \left(\frac{nM^2}{A}\right)^{3/2}\left(\frac{\rho_s}{\rho_f}\right) \quad (1)$$

where n, M, and A are the number of cells in the micrograph, the magnification of the micrograph, and the area of the micrograph (cm^2), respectively. The densities of solid (ρ_s) and foamed (ρ_f) samples were evaluated via a water-displacement method (ASTM D792).

2.3.2. Thermal Analysis. The thermal diffusivity (α) of the composite foams was determined by the laser method using an LFA-467 (NETZSCH, Germany) at 20 °C. The dimensions of the samples were 25 mm × 4 mm (diameter and height, respectively). Three measurements were taken for each sample to obtain statistical data.

2.3.3. Compression Testing. Compressive tests according to the ISO 604:2002 standard were made in a universal testing machine (Shenzhen SANA, China) with a crosshead speed of 1 mm/min. Specimen dimensions for compressive testing were 10 mm × 10 mm × 4 mm. The compressive loading direction was horizontal to the interface between adjacent layers. All measurements were repeated at least five times, and the average values were reported.

2.3.4. Dynamic Mechanical Analysis. Dynamic mechanical analysis (Q500, TA) of epoxy composite foams was performed using a three-point bending configuration with a span distance of 20 mm and an oscillation frequency of 1 Hz. Specimen dimensions were 30 mm × 10 mm × 4 mm. A multistrain sweep mode was adopted. The amplitude range was 1−25 μm, and the measured temperature was fixed at 30 °C

2.3.5. Electrical Conductivity Measurement. The square resistance of the outside layer of EP/MWCNT foams was measured by a four-point-probe instrument (FT331, China). When the square resistance of composite foams was higher than 2×10^5 Ω/□ (limit value), the surface resistivity instead of square resistance was measured by a super megohm meter (SM7110, Hioki, Japan). The diameter of the samples was 35.5 mm. Three measurements were taken for each sample to obtain statistical data.

2.3.6. EMI Shielding Measurement. The EMI shielding effectiveness (EMI SE) was determined using an Agilent N5234A vector network analyzer in the frequency range of 8.2−12.4 GHz (X-band). The dimensions of the rectangular samples were 22 × 10.5 × 4 mm^3. The scattering parameters (S_{11}, S_{21}) were recorded to calculate the reflected power (R), transmitted power (T), total EMI SE (SE_T), microwave reflection (SE_R), and microwave absorption (SE_A) based on eqs 2−5.[25,26]

$$R = |S_{11}|^2,\ T = |S_{21}|^2 \quad (2)$$

$$SE_R = 10\lg\left(\frac{1}{1-R}\right) \quad (3)$$

$$SE_A = 10\lg\left(\frac{1-R}{T}\right) \quad (4)$$

$$SE_T = SE_R + SE_A \quad (5)$$

3. RESULTS AND DISCUSSION

3.1. Cell Morphology. Figure 2 shows the morphology of the monolayer EP/MWCNT foams with different MWCNT or CFA contents. Closed cellular structures were observed in all of the composite foams, and the cell morphology was affected by both MWCNT and CFA contents (Figure 5). On the one hand, EP/MWCNT foams loaded with 0.5 wt % MWCNT had an average cell diameter of 26.54 μm and a cell density of 5.63 × 10^7 cells/cm^3. With increasing the MWCNT content to 2.0 wt %, the average cell size decreased to 24.20 μm and the cell density increased to 8.17 × 10^7 cells/cm^3. This result can be attributed to the well-known heterogeneous nucleation effect of nanoparticles.[19,23] Due to the lower activation energy barrier for nucleation, cell nucleation readily took place in the boundary between the epoxy matrix and the MWCNTs, and then small bubbles appeared. A higher MWCNT content provided more nucleating sites, which was beneficial to the improvement of cell morphology. In addition, the viscoelasticity of the composites could increase with the increased MWCNT content, which facilitated cell stability to obtain small bubbles.[23] On the other hand, when the CFA content increased from 0.5 to 1.5 wt %, the cell size decreased from 24.20 to 21.06 μm and the cell density increased from 8.17 × 10^7 to 1.33 × 10^8 cells/cm^3 (Figure 2b,c). This observation was due to the fact that the foaming process was conducted in a limited space. When the mold was completely filled with the foaming material, cell growth was restricted and arrested during foaming, leading to a short growth time of bubbles.[24,27] Short growth time, in turn, reduced the coalescence and rupture of bubbles. An increase in the CFA content led to increased cell nucleation and a fast expansion rate of samples,

https://doi.org/10.1021/acsomega.2c02710
ACS Omega 2022, 7, 33010−33018

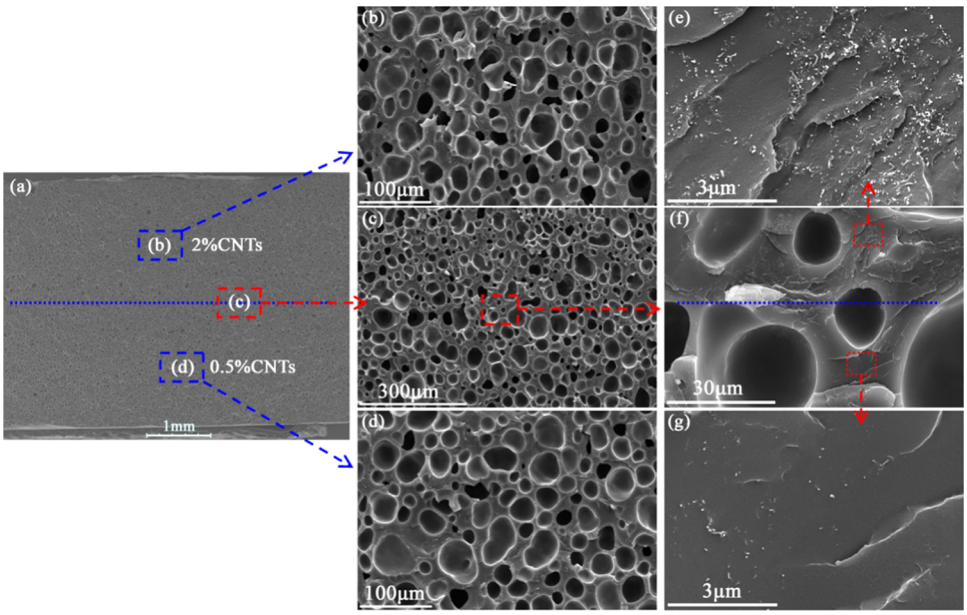

Figure 3. Typical SEM micrographs of the two-layer composite foam (EP/CNT-0.5/2): (a) whole fractured surface, (b, e) layer with 2 wt % MWCNT, (c, f) interface between layers, and (d, g) layer with 0.5 wt % MWCNT.

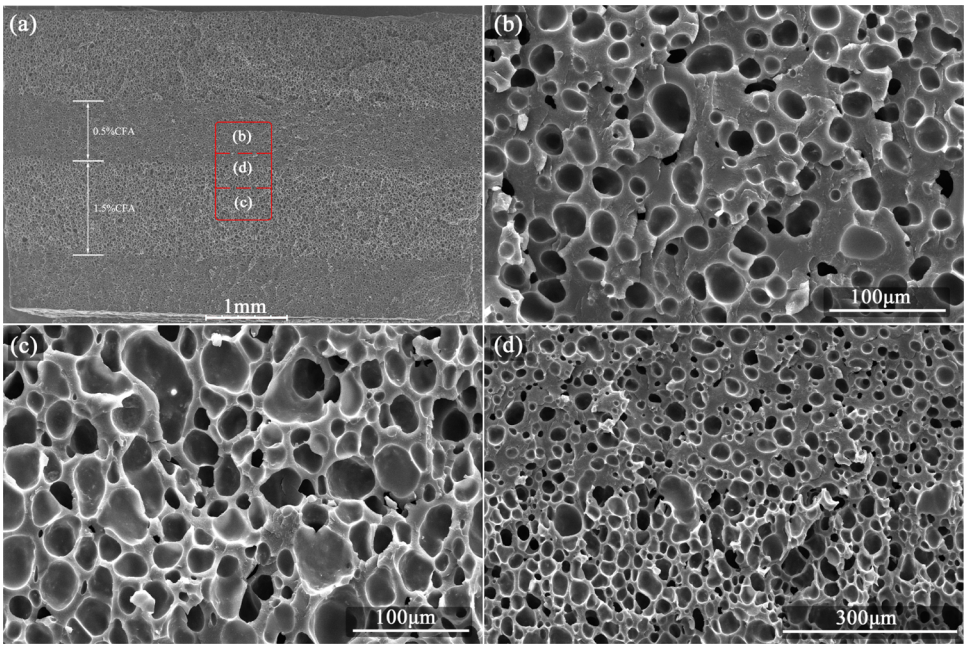

Figure 4. Typical SEM micrographs of four-layer epoxy foams (EP/CFA-0.5/1.5): (a) whole fractured surface, (b) layer with 0.5 wt % CFA, (c) layer with 1.5 wt % CFA, and (d) interface between layers.

thus shortening the growth time of bubbles and then resulting in a smaller cell size.

Two kinds of hybrid powders loaded with 0.5 and 2.0 wt % MWCNT were compressed layer by layer to prepare two- and four-layer composites. Figure 3 shows the representative SEM images (two-layer) of the resulting laminated epoxy foams. The cell morphology parameters, including cell size and cell density, are presented in Figure 5a. The cell size in the top layer containing 2 wt % MWCNT was smaller than that in the bottom layer with 0.5 wt % MWCNT, and the cell density in the top layer was higher (Figure 3a–d). As shown in Figure 5a, the cell morphology of each layer in two- and four-layer composite foams corresponded with the structure of the monolayer foams, indicating that the foaming behavior was not affected by the multilayer structure. This result was attributed to the relatively large layer thickness. If the layer thickness further decreased, the cell size of multilayered foams could decrease.[14,16] The interface between these two layers can be hardly distinguished from the low-magnification SEM picture (Figure 3a) but it can be clearly distinguished from the high-magnification SEM picture due to the difference in the MWCNT content (Figure 3e–g). Lots of agglomerated MWCNTs in the upper layer constructed the conductive networks within the epoxy matrix (Figure 3e), while few isolated nanotubes or MWCNT agglomerates dispersed in the matrix were observed in the bottom layer (Figure 3g). The

https://doi.org/10.1021/acsomega.2c02710
ACS Omega 2022, 7, 33010−33018

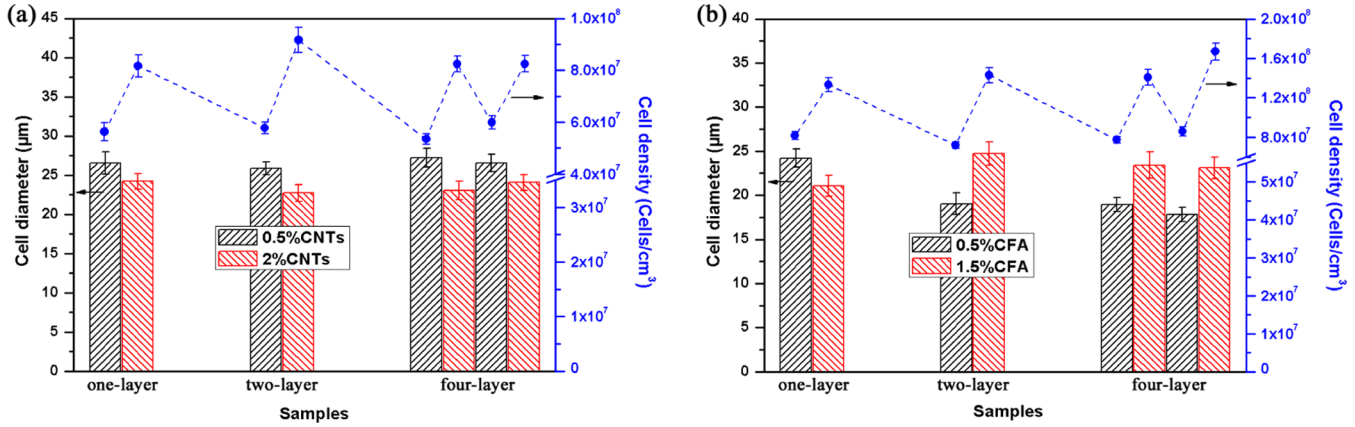

Figure 5. Cell size and cell density of epoxy foams with different (a) MWCNT contents and (b) CFA contents.

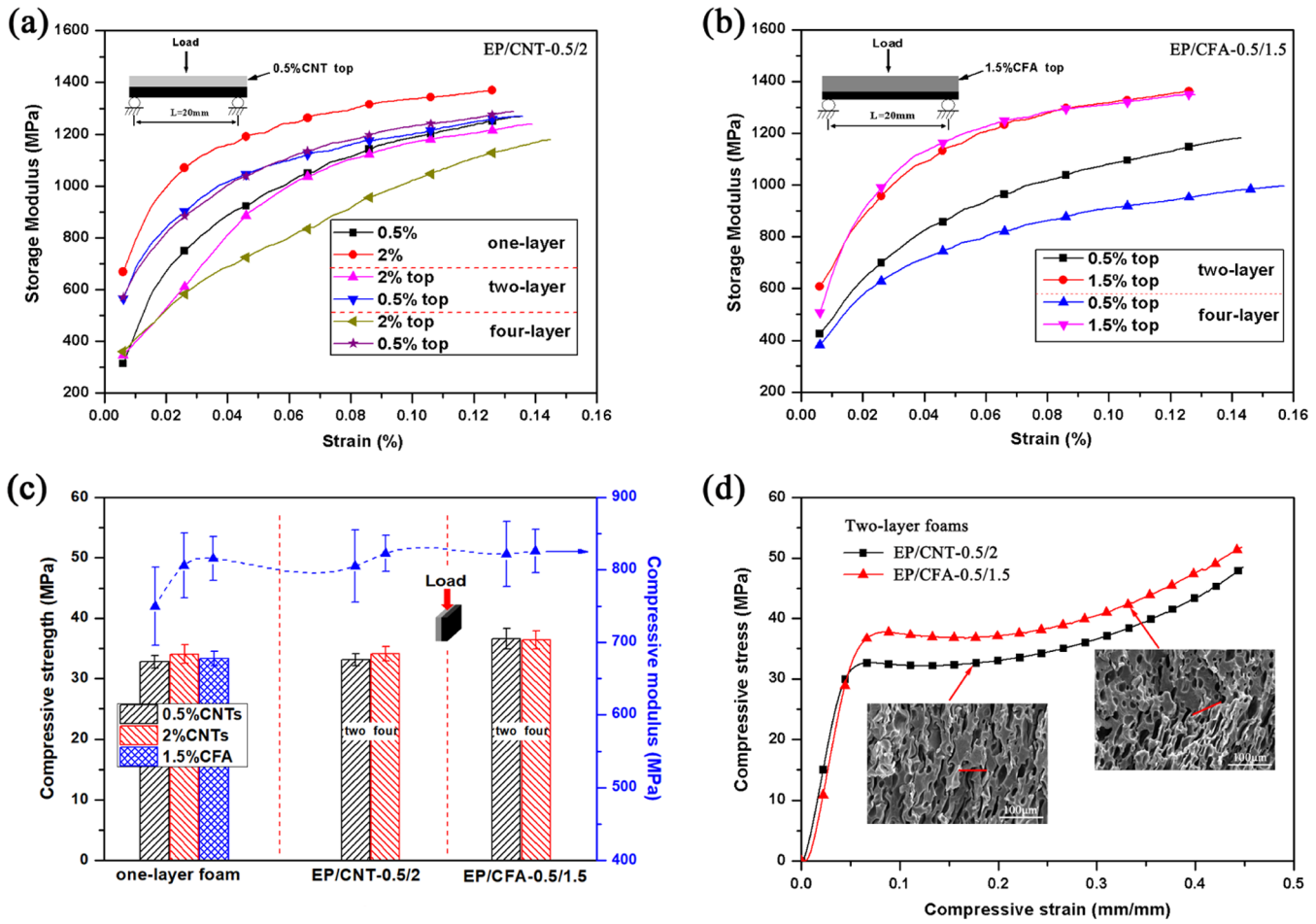

Figure 6. Storage modulus of different composite foams with different (a) MWCNT contents and (b) CFA contents, (c) compressive strength and modulus of composite foams, and (d) typical compressive stress−strain curve and SEM pictures.

blue dashed line in Figure 3a represents the interface of the laminated composite foam. It can be found that the thickness of each layer in the two-layer foam was the same, indicating the same density of each layer. The same observation was also found in the four-layer foams. Moreover, the interface of the two-layer foam was continuous after curing (Figure 3f), indicating strong interface bonding strength.

Two kinds of hybrid powders loaded with 0.5 and 1.5 wt % CFA were compressed layer by layer to prepare two- and four-layer composites. The typical SEM images (four-layer) of the resulting laminated epoxy foams are shown in Figure 4. The cell morphology parameters are presented in Figure 5b. A larger cell size and a higher cell density were observed in the layers with 1.5 wt % CFA (Figure 4a,c) in contrast to the layers with 0.5 wt % CFA (Figure 4a,b), which was different from the observation of corresponding monolayer foams (Figure 3b,c). This result was due to the difference in the expansion rate between layers with different CFA contents. A higher CFA content produced more gas and then led to a larger volume expansion of the corresponding layer, thus squeezing the

https://doi.org/10.1021/acsomega.2c02710
ACS Omega 2022, 7, 33010−33018

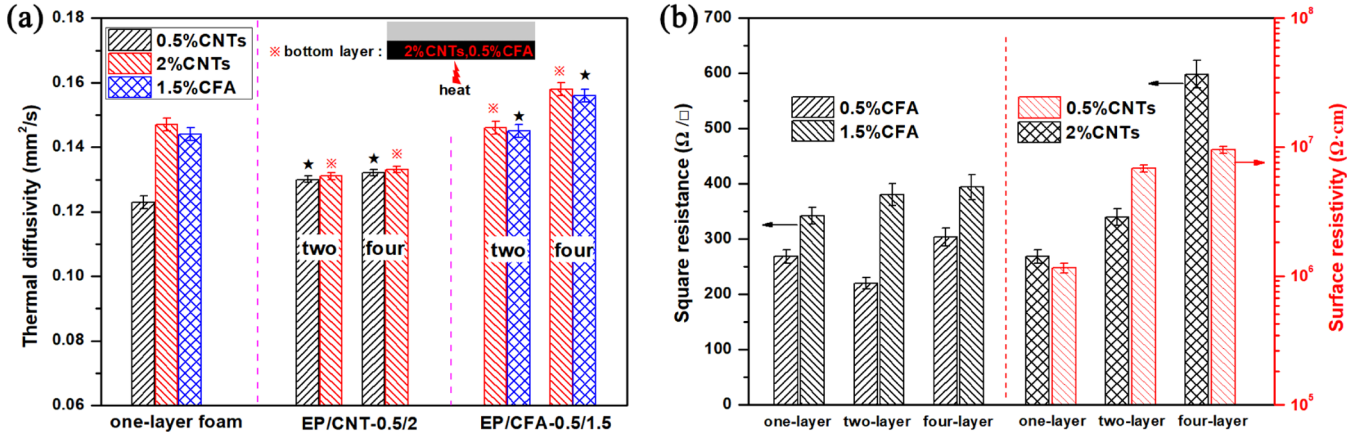

Figure 7. (a) Thermal diffusivity and (b) electrically conductive properties of different foams.

foaming space of the layer with lower CFA content in a laminated sample. Therefore, the layers with higher CFA content in the multilayered composite foams presented larger cell size, higher cell density, and wider layer thickness. As inferred from Figure 4a, the thickness of the layers with 1.5 wt % CFA was about 1.5 times thicker than that of the layers with 0.5 wt % CFA. It meant that the density of the layers with 1.5 wt % CFA was 1.5 times lower than that of the layers with 0.5 wt % CFA. Combined with the density value of multilayered foams (0.713 g/cm^3), it can be calculated that the density of layers with 0.5 and 1.5 wt % CFA was 0.891 and 0.594 g/cm^3, respectively. The same observation was also found in the two-layer foams. In addition, a continuous interface with perfect bonding between adjacent layers was clearly distinguished from the SEM pictures (Figure 4a,d).

3.2. Compressive and Dynamic Mechanical Properties. The storage modulus of different epoxy foams as a function of strain at 30 °C is shown in Figure 6a,b. The storage modulus is an important parameter reflecting the stiffness of materials. It can be seen that the storage modulus increased first and then gradually leveled off with increasing the strain. Monolayer composite foams loaded with 2 wt % MWCNT had a higher storage modulus value compared with composite foams containing 0.5 wt % MWCNT (Figure 6a), indicating higher stiffness of the composite foams with higher MWCNT content. This result can be attributed to the strengthening effect of MWCNT.[28] However, for the multilayered composite foams (EP/CNT-0.5/2), the storage modulus was extremely dependent on the loading direction, which was due to the significant difference between outside layers of the same sample. When the layer with 2 wt % MWCNT was far away from the stress surface (bottom), the storage modulus value of the multilayered foams was between that of the corresponding two kinds of monolayer foams, which was in agreement with the mixture rule of two-phase composite. In contrast, when the layer with 2 wt % MWCNT was close to the stress surface (top), the storage modulus value of the multilayered foams was even lower than that of the monolayer foams containing 0.5 wt % MWCNT. As is known, during flexure, the bubbles in the composite foams beneath the loading cell will undergo local compression, whereas the bubbles on the opposite side will tend to stretch.[29,30] The results inferred from Figure 6a indicated that the tensile side was under a relatively large load, and thereby the multilayered composite foams exhibit a high stiffness when the layer with high stiffness was placed on the tensile side. In addition, the layer number had an important influence on the storage modulus of multilayered composite foams only when the layer with low stiffness was placed on the tensile side. In this case, the storage modulus of the four-layer composite foam was lower than that of the two-layer foam. This situation can be related to the decreased thickness of the layer, which further reduced the stiffness of the weaker layer on the tensile side. As shown in Figure 6b, the storage modulus of multilayered composite foams with different CFA contents (EP/CFA-0.5/1.5) exhibited a similar tendency, that was, the multilayered foams presented a high storage modulus when the layer containing 0.5 wt % CFA was placed on the tensile side (bottom). It should be noted that the layer with 0.5 wt % CFA, in contrast to the layer with 1.5 wt % CFA, exhibited a higher storage modulus due to the smaller cell size and higher density.[24]

Because of the difference in properties between adjacent layers, the multilayered composite foams showed different storage modulus values at different loading directions when the loading direction was vertical to the interface. When the loading direction was horizontal to the interface, the compressive properties of different epoxy foams were investigated, as shown in Figure 6c. The compressive yield strength and the modulus of the monolayer composite foam with 0.5 wt % CNT were 32.75 and 749.73 MPa, respectively, while those of the monolayer foam with 2 wt % CNT increased to 34.04 and 806.26 MPa, respectively. For the multilayered composite foams (EP/CNT-0.5/2), the compressive strength and modulus of four-layer foams were slightly higher than those of two-layer foams, and their compressive properties were close to those of the monolayer composite foam with 2 wt % MWCNT. This result indicated that layers with high compressive properties can act as the framework material to endow multilayered foams with excellent compressive properties. On the other hand, the compressive strength and the modulus of both two-layer and four-layer foams (EP/CFA-0.5/1.5) were about 36.5 and 823 MPa, respectively, which were mildly higher than those of the monolayer composite foam with 0.5 wt % CFA. This was because the layer with 0.5 wt % CFA in the multilayered foams, in contrast to the corresponding monolayer foam, must have higher compressive properties due to its higher density.[16,24,26] Figure 6d shows the typical compressive stress−strain curves of two-layer composite foams. Although bubbles are seriously distorted at a strain of 45%, the intact interface without delamination and smooth

https://doi.org/10.1021/acsomega.2c02710
ACS Omega 2022, 7, 33010−33018

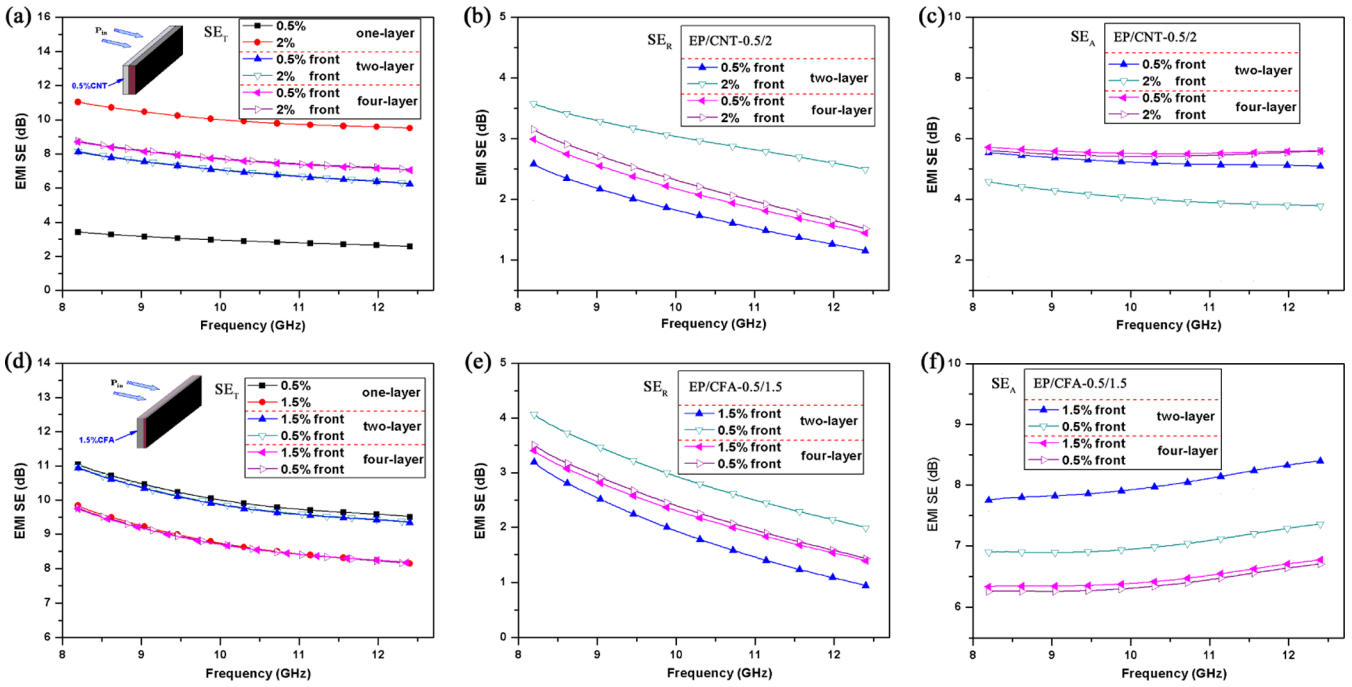

Figure 8. EMI SE_T, SE_R, and SE_A of composite foams with different (a−c) CNT contents and (d−f) CFA contents.

stress−strain curves are shown in Figure 6d, which illustrates the strong interface bonding strength between layers. The strong interface bonding strength, in turn, significantly enhanced the load-bearing capacity of the multilayered composite foam, even though the loading direction was horizontal to the interface.

3.3. Electrically and Thermally Conductive Properties. Figure 7a shows the thermal diffusivity of different composite foams. As the MWCNT content increased from 0.5 to 2 wt %, the thermal diffusivity of monolayer foams increased from 0.123 to 0.147 mm^2/s, which was attributed to the superhigh thermal conductive properties of MWCNT.[8,31] When the CFA content increased to 1.5 wt %, the thermal diffusivity of monolayer foams slightly decreased to 0.144 mm^2/s, which was due to the decreased cell size. For multilayered composite foams (EP/CNT-0.5/2), the thermal diffusivity of multilayered composite foams was between that of the corresponding monolayer foams, satisfying the mixture rule. However, the thermal diffusivity of the multilayered EP/CFA-0.5/1.5 foam was even higher than that of the monolayer foams, and the maximum value reached up to 0.158 mm^2/s. This result was due to the presence of a high-density layer with 0.5 wt % CFA (0.891 g/cm^3) in the EP/CFA-0.5/1.5 foam. A high density could enhance the solid-phase thermal conduction of the composite foam[24] and thus increase the thermal conductive property of multilayered composite foams. In addition, the thermal diffusivity of multilayered foams increased with the increase in the layer number, resulting in the thermal diffusivity of multilayered foams shifting near to that of the layer with higher thermal diffusivity. This result can possibly be related to the decreased interface spacing between layers with high thermal diffusivity. When the layer with high thermal diffusivity (layer containing 2 wt % CNT and 0.5% CFA) suffered from heat first, the thermal diffusivity of multilayered composite foams was relatively higher, indicating that the thermally conductive pathway had an influence on the thermal conductive properties.

The electrically conductive properties of the composite foams are shown in Figure 7b. For composite foams with different MWCNT contents, with the layer number increased, the surface resistivity of the layer containing 0.5 wt % MWCNT increased, and simultaneously the square resistance of the layer with 2 wt % MWCNT also increased. As previously reported,[24] the limited-foaming process led to an increase in the electrical resistance of the epoxy foam in comparison with the free-foaming process, which can be attributed to the fact that the short growth time of bubbles reduced the time for MWCNTs to redistribute, and the straining molecular chains hindered the movement of MWCNTs to reconstruct the interconnections between MWCNTs. As a result, as the layer number increased, the layer thickness reduced, and thus the degree of restriction during foaming increased. The increased degree of restriction, in turn, further hindered the movement of MWCNT, consequently increasing the electrical resistance of each layer in the multilayered composite foams. However, compared with composite foams containing different MWCNT contents, the change in the square resistance for composite foams containing different CFA contents was different, that was, the square resistance of the layer with 0.5 wt % CFA reduced first and then increased as the layer number increased from one to four. The decreased process of square resistance was attributed to the increased density of this layer.[24,26,32] In addition, in contrast to the extremely different electrically conductive properties between adjacent layers in EP/CNT-0.5/2 foams, the difference in square resistance between adjacent layers in EP/CFA-0.5/1.5 foams can be even ignored. This was because the difference in electrical resistance between adjacent layers in EP/CNT-0.5/2 foams was induced by the cell morphology, while that in EP/CFA-0.5/1.5 foams was mainly induced by the MWCNT content.

When the MWCNT content increased from 0.5 to 2 wt %, the electrically conductive properties of composite foams increased significantly, whereas the thermal diffusivity only mildly increased. This result was attributed to the different

https://doi.org/10.1021/acsomega.2c02710
ACS Omega 2022, 7, 33010−33018

mechanisms of electrical conduction and thermal conduction.[7,8,24,25] The electrical conduction was mainly contributed by electron transport along the conductive pathway. When 2 wt % MWCNT was added, a perfect CNT network in the epoxy matrix was formed, and thus the composite foam with excellent electrical properties was obtained. However, although the MWCNT had a superhigh thermal conductivity (~3000 W/m·K), the composite foam with 2 wt % MWCNT still exhibited a low thermal diffusivity. This result was ascribed to the fact that the thermal conduction relied on phonon propagation among the composite. Due to the different phonon spectra between the MWCNT and the polymer, a high interfacial thermal resistance between the CNT−polymer caused strong phonon scattering, leading to poor thermal conduction.[8,24]

3.4. EMI Shielding Properties. The EMI shielding effectiveness (SE) of these two series of composite foams over the X-band frequency range (8.2−12.4 GHz) is measured, and the results are shown in Figure 8. As indicated in Figure 8a,d, the total EMI SE (SE_T) of all composite foams was relatively frequency-dependent and decreased gradually with increasing frequency. The average SE_T values of the two-layer and four-layer composite foams (EP/CNT-0.5/2) were about 7.2 and 7.9 dB, respectively, which were between those of the corresponding monolayer composite foams with different MWCNT contents (Figure 8a). The larger impedance mismatch between adjacent layers could improve the multiple interfacial reflection of electromagnetic microwave (EMW), thus making the re-reflected waves get absorbed or dissipated in the form of heat within the porous material and resulting in a great enhancement in the absorption or dissipation of EMW in the layer with high electrical conductivity.[11,25] As a result, the increased number of interfaces led to a higher SE_T of four-layer foams. On the contrary, as shown in Figure 8d, the average SE_T value of the two-layer composite foams (EP/CFA-0.5/1.5) was about 10.1 dB, which was higher than that of the four-layer foams (8.9 dB). This result can be attributed to two factors: (a) the increased electrical resistance of four-layer foams decreased EMW attenuation due to the reduced conductive loss.[6,23] (b) The poor impedance mismatch between adjacent layers weakened the interfacial reflection of EMW.

The SE_T of multilayered composite foams was not affected by the direction of the incident EMW. However, the SE_R and SE_A of the multilayered foams were quite different at different incident EMW directions. For a certain multilayered foam (EP/CNT-0.5/2), the SE_R was lower, whereas the SE_A was higher when the incident EMW first encountered the layer with 0.5 wt % MWCNT (Figure 8b,c). Similarly, when the incident EMW first encountered the layer containing 1.5 wt % CFA, the multilayered composite foam (EP/CFA-0.5/1.5) presented a lower SE_R but a higher SE_A (Figure 8e,f). These results indicated that the multilayered foams presented a stronger microwave-absorbing ability when the outside layer with lower electrical conductivity first faced the incident EMW, which was in agreement with the results of previous studies.[12] This situation was mainly due to the laminated structure, which reduced the microwave reflectivity in the front layer while simultaneously improving the microwave loss in the back layer with high electrical conductivity.[11,12,33] However, the difference in SE_R or SE_A caused by the direction of incident EMW largely narrowed as the layer number increased from two to four, indicating that the anisotropy of the composite foams with the alternating layer structure could be weakened by increasing the layer number. In addition, as shown in Figure 8f, the four-layer composite foams (EP/CFA-0.5/1.5) exhibited a lower SE_A in comparison with the two-layer foams. It meant that the increase in the interfacial number did not always enhance the absorption of EMW for the multilayered foams, although the cell morphology and density between adjacent layers were extremely different.

4. CONCLUSIONS

In this work, microcellular epoxy/multiwalled carbon nanotube (EP/MWCNT) composite foams with an alternating layer structure were prepared through the combination of multilayer powder pressing and chemical foaming technology. The same density and layer thickness but different cell morphologies and electrical conductivities between adjacent layers in the multilayer foams (two- and four-layer) were found when the adjacent layers were loaded with 0.5 and 2 wt % MWCNT, respectively. Similar electrical conductivity but different cell morphologies, densities, and layer thicknesses between adjacent layers in the multilayer foams were obtained when the adjacent layers were added 0.5 and 1.5 wt % CFA, respectively. For these two series of multilayered composite foams with different structures, the effect of the layer number and the loading direction on the compressive properties, storage modulus, and thermal diffusivity showed a similar tendency, while the change in electromagnetic interference shielding properties was different. This work provides a valuable guide for designing the microstructures between adjacent layers for different applications.

AUTHOR INFORMATION

Corresponding Author

Shaohua Sun − *Naval University of Engineering, Wuhan 430033 Hubei, China;* orcid.org/0000-0003-2305-9702; Email: happysunshao@163.com

Authors

Lijun Wang − *National Engineering Research Center for Compounding and Modification of Polymer Materials, Guizhou Material Industrial Technology Institute, Guiyang 550014 Guizhou, China*

Bin Xue − *National Engineering Research Center for Compounding and Modification of Polymer Materials, Guizhou Material Industrial Technology Institute, Guiyang 550014 Guizhou, China*

Complete contact information is available at: https://pubs.acs.org/10.1021/acsomega.2c02710

Notes

The authors declare no competing financial interest.

ACKNOWLEDGMENTS

The authors greatly appreciate the financial support from the National Nature Science Foundation of China (Nos. 51963005 and 51503047), the Multi-level Talent Program of Guizhou Province ([2019]5631), and the Research Institution Service Enterprise Project of Guizhou Province ([2018]4010).

REFERENCES

(1) Sandler, J. K. W.; Kirk, J. E.; Kinloch, I. A.; Shaffer, M. S. P.; Windle, A. H. Ultra-low electrical percolation threshold in carbon-nanotube-epoxy composites. *Polymer* **2003**, *44*, 5893−5899.

https://doi.org/10.1021/acsomega.2c02710
ACS Omega 2022, 7, 33010−33018

(2) Bryning, M. B.; Islam, M. F.; Kikkawa, J. M.; Yodh, A. G. Very low conductivity threshold in bulk isotropic single-walled carbon nanotube−epoxy composites. *Adv. Mater.* **2005**, *17*, 1186−1191.
(3) Zhang, W.; Dehghani-Sanij, A. A.; Blackburn, R. S. Carbon based conductive polymer composites. *J. Mater. Sci.* **2007**, *42*, 3408−3418.
(4) Baughman, R. H.; Zakhidov, A. A.; De Heer, W. A. Carbon nanotubes-the route toward applications. *Science* **2002**, *297*, 787−792.
(5) Hao, B.; Mu, L.; Ma, Q.; Yang, S.; Ma, P. C. Stretchable and compressible strain sensor based on carbon nanotube foam/polymer nanocomposites with three-dimensional networks. *Compos. Sci. Technol.* **2018**, *163*, 162−170.
(6) Zhang, H. B.; Yan, Q.; Zheng, W. G.; He, Z.; Yu, Z. Z. Tough graphene− polymer microcellular foams for electromagnetic interference shielding. *ACS Appl. Mater. Interfaces* **2011**, *3*, 918−924.
(7) Zhou, M.; Zhu, W.; Yu, S.; Tian, Y.; Zhou, K. Selective laser sintering of carbon nanotube−coated thermoplastic polyurethane: Mechanical, electrical, and piezoresistive properties. *Composites, Part C* **2022**, *7*, No. 100212.
(8) Yuan, S.; Zheng, Y.; Chua, C. K.; Yan, Q.; Zhou, K. Electrical and thermal conductivities of MWCNT/polymer composites fabricated by selective laser sintering. *Composites, Part A* **2018**, *105*, 203−213.
(9) Wang, L.; Yang, B.; Zhou, L.; Xue, B.; Yang, Z. Evolution of anisotropic bubbles and transition of the mechanical and electrical properties during a non-continuous two-step foaming of epoxy/carbon nanofiber composites. *Compos. Sci. Technol.* **2021**, *213*, No. 108918.
(10) Wang, S.; Huang, Y.; Zhao, C.; Chang, E.; Ameli, A.; Naguib, H. E.; Park, C. B. Theoretical modeling and experimental verification of percolation threshold with MWCNTs' rotation and translation around a growing bubble in conductive polymer composite foams. *Compos. Sci. Technol.* **2020**, *199*, No. 108345.
(11) Yuan, H.; Xiong, Y.; Shen, Q.; Luo, G.; Zhou, D.; Liu, L. Synthesis and electromagnetic absorbing performances of CNTs/PMMA laminated nanocomposite foams in X-band. *Compostes, Part A* **2018**, *107*, 334−341.
(12) Li, Y.; Shen, B.; Yi, D.; Zhang, L.; Zhai, W.; Wei, X.; Zheng, W. The influence of gradient and sandwich configurations on the electromagnetic interference shielding performance of multilayered thermoplastic polyurethane/graphene composite foams. *Compos. Sci. Technol.* **2017**, *138*, 209−216.
(13) Han, T.; Wang, X.; Xiong, Y.; Li, J.; Guo, S.; Chen, G. Lightweight poly (vinyl chloride)-based soundproofing composites with foam/film alternating multilayered structure. *Composites, Part A* **2015**, *78*, 27−34.
(14) Zhao, T.; Yang, M.; Wu, H.; Guo, S.; Sun, X.; Liang, W. Preparation of a new foam/film structure poly (ethylene-co-octene) foam materials and its sound absorption properties. *Mater. Lett.* **2015**, *139*, 275−278.
(15) Xu, S.; Wen, M.; Li, J.; Guo, S.; Wang, M.; Du, Q.; Shen, J.; Zhang, Y.; Jiang, S. Structure and properties of electrically conducting composites consisting of alternating layers of pure polypropylene and polypropylene with a carbon black filler. *Polymer* **2008**, *49*, 4861−4870.
(16) Zhou, D.; Xiong, Y.; Yuan, H.; Luo, G.; Zhang, J.; Shen, Q.; Zhang, L. Synthesis and compressive behaviors of PMMA microporous foam with multi-layer cell structure. *Composites, Part B* **2019**, *165*, 272−278.
(17) Sumey, J. L.; Sarver, J. A.; Kiran, E. Foaming of polystyrene and poly (methyl methacrylate) multilayered thin films with supercritical carbon dioxide. *J. Supercrit. Fluids* **2019**, *145*, 243−252.
(18) Fan, X.; Zhang, G.; Gao, Q.; Li, J.; Shang, Z.; Zhang, H.; Zhang, Y.; Shi, X.; Qin, J. Highly expansive, thermally insulating epoxy/Ag nanosheet composite foam for electromagnetic interference shielding. *Chem. Eng. J.* **2019**, *372*, 191−202.
(19) Fan, X.; Zhang, G.; Li, J.; Shang, Z.; Zhang, H.; Gao, Q.; Qin, J.; Shi, X. Study on foamability and electromagnetic interference shielding effectiveness of supercritical CO_2 foaming epoxy/rubber/MWCNTs composite. *Composites, Part A* **2019**, *121*, 64−73.
(20) Duan, H.; Zhu, H.; Yang, J.; Gao, J.; Yang, Y.; Xu, L.; Zhao, G.; Liu, Y. Effect of carbon nanofiller dimension on synergistic EMI shielding network of epoxy/metal conductive foams. *Composites, Part A* **2019**, *118*, 41−48.
(21) Yang, J.; Yang, Y.; Duan, H.; Zhao, G.; Liu, Y. Light-weight epoxy/nickel coated carbon fibers conductive foams for electromagnetic interference shielding. *J. Mater. Sci.: Mater. Electron.* **2017**, *28*, 5925−5930.
(22) Smorygo, O.; Mikutski, V.; Marukovich, A.; Sadykov, V.; Bespalko, Y.; Stefan, A.; Pelin, C. E. Preparation and characterization of open-cell epoxy foams modified with carbon fibers and aluminum powder. *Compos. Struct.* **2018**, *202*, 917−923.
(23) Li, J.; Zhang, G.; Ma, Z.; Fan, X.; Fan, X.; Qin, J.; Shi, X. Morphologies and electromagnetic interference shielding performances of microcellular epoxy/multi-wall carbon nanotube nanocomposite foams. *Compos. Sci. Technol.* **2016**, *129*, 70−78.
(24) Wang, L.; He, Y.; Jiang, T.; Zhang, X.; Zhang, C.; Peng, X. Morphologies and properties of epoxy/multi-walled carbon nanotube nanocomposite foams prepared through the free-foaming and limited-foaming process. *Compos. Sci. Technol.* **2019**, *182*, No. 107776.
(25) Jin, X.; Wang, J.; Dai, L.; Liu, X.; Li, L.; Yang, Y.; Cao, Y.; Wang, W.; Wu, H.; Guo, S. Flame-retardant poly (vinyl alcohol)/MXene multilayered films with outstanding electromagnetic interference shielding and thermal conductive performances. *Chem. Eng. J.* **2020**, *380*, No. 122475.
(26) Feng, D.; Liu, P.; Wang, Q. Exploiting the piezoresistivity and EMI shielding of polyetherimide/carbon nanotube foams by tailoring their porous morphology and segregated CNT networks. *Composites, Part A* **2019**, *124*, No. 105463.
(27) Wang, L.; Zhang, C.; Gong, W.; Ji, Y.; Qin, S.; He, L. Preparation of Microcellular Epoxy Foams through a Limited-Foaming Process: A Contradiction with the Time−Temperature−Transformation Cure Diagram. *Adv. Mater.* **2018**, *30*, No. 1703992.
(28) Kuang, T.; Chang, L.; Chen, F.; Sheng, Y.; Fu, D.; Peng, X. Facile preparation of lightweight high-strength biodegradable polymer/multi-walled carbon nanotubes nanocomposite foams for electromagnetic interference shielding. *Carbon* **2016**, *105*, 305−313.
(29) Karthikeyan, C. S.; Sankaran, S.; et al. Investigation of bending modulus of fiber-reinforced syntactic foams for sandwich and structural applications. *Polym. Adv. Technol.* **2007**, *18*, 254−256.
(30) Wang, L.; Zhang, J.; Yang, X.; Zhang, C.; Gong, W.; Yu, J. Flexural properties of epoxy syntactic foams reinforced by fiberglass mesh and/or short glass fiber. *Mater. Des.* **2014**, *55*, 929−936.
(31) Han, Z.; Fina, A. Thermal conductivity of carbon nanotubes and their polymer nanocomposites: A review. *Prog. Polym. Sci* **2011**, *36*, 914−944.
(32) Xu, X. B.; Li, Z. M.; Shi, L.; Bian, X. C.; Xiang, Z. D. Ultralight Conductive Carbon-Nanotube−Polymer Composite. *Small* **2007**, *3*, 408−411.
(33) Sheng, A.; Ren, W.; Yang, Y.; Yan, D. X.; Duan, H.; Zhao, G.; Liu, Y.; Li, Z. M. Multilayer WPU conductive composites with controllable electro-magnetic gradient for absorption-dominated electromagnetic interference shielding. *Composites, Part A* **2020**, *129*, No. 105692.

https://doi.org/10.1021/acsomega.2c02710
ACS Omega 2022, 7, 33010−33018